Asian Journal of Research and Reviews in Physics

Volume 7, Issue 1, Page 33-56, 2023; Article no.AJR2P.98200
ISSN: 2582-5992

Fluid and Lithology Discrimination for Reservoir Characterization of HAX Field, Offshore Niger Delta

E. V. Umeadi [a] and A. O. Balogun [a*]

[a] Department of Physics, University of Port Harcourt, Rivers, Nigeria.

Authors' contributions

This work was carried out in collaboration between both authors. Both authors read and approved the final manuscript.

Article Information

DOI: 10.9734/AJR2P/2023/v7i1133

Open Peer Review History:
This journal follows the Advanced Open Peer Review policy. Identity of the Reviewers, Editor(s) and additional Reviewers, peer review comments, different versions of the manuscript, comments of the editors, etc are available here: https://www.sdiarticle5.com/review-history/98200

Original Research Article

Received: 02/02/2023
Accepted: 04/04/2023
Published: 15/04/2023

ABSTRACT

Fluid and lithology discrimination for reservoir characterization of HAX field, offshore Niger Delta was carried out in this study. Three reservoir intervals, R_4500, R_5500, and R_6500 were picked, identified, and correlated across the four wells; but only the R_5500 reservoir was analyzed. The cross-plot analysis of elastic rock properties with reservoir properties such as Vp/Vs ratio against Acoustic Impedance, Lambda-Rho against Vp/Vs, Mu-Rho against Density, and Lambda-Rho against Mu-Rho colour-coded by gamma ray, water saturation, and density respectively was carried out for fluid and lithology discrimination. The result of these elastic rock properties when colour-coded with gamma ray distinguished reservoir R_5500 into the sand zone and shale zone for the four wells, these results depict lithology discrimination as predominantly found in the Niger Delta basin. Consequently, when colour–coded by water saturation reservoir R_5500 was distinguished into three zones namely the hydrocarbon bearing zone, brine sand zone and shale zone indicative of both lithology and fluid discrimination. From these cross-plots, the clusters with the least water saturation correspond to highly charged hydrocarbon saturation sand while clusters with maximum water saturation correspond to non-hydrocarbon zone (brine sand and shale).

**Corresponding author: E-mail: ayomide.balogun@uniport.edu.ng;*

Finally, when colour–coded by density reservoir R_5500 was distinguished into four zones namely gas sand zone and oil sand zone, brine sand zone, and shale zone indicating fluid types. The result shows relatively lower Acoustic Impedance, Vp/Vs ratio, lambda-rho, mu-rho, and density (as the colour-code) values indicating hydrocarbon bearing sand while the relatively higher Acoustic Impedance, Vp/Vs ratio, lambda-rho, mu-rho and density (as the colour-code) values are associated with non-hydrocarbon zone (shale and brine sand). This study has been able to discriminate hydrocarbon reservoirs using the cross-plots of elastic rock properties in the zone of interest and proven that the HAX field is viable in terms of hydrocarbon prospects and highly economical for production.

Keywords: Lithology discrimination; fluid discrimination cross-plot analysis; elastic property.

1. INTRODUCTION

"The economic viability of a hydrocarbon field is reliant on the quality, quantity, and accuracy of lithology and pore fluid" [1]. "Accurate description, evaluation, and prediction of a reservoir in terms of lithology and fluid content is an important factor in reducing the risk involved in hydrocarbon exploitation and exploration" [2,3]. "There has been a growing interest in determining lithology and pore fluid using well log data, which is cheaper, more reliable, and economical. Well logging offers the benefit of covering the entire geological formation of interest coupled with providing general and excellent details of the underground formation" [4]. According to [5], "well logs offer a better representation of in-situ conditions in a lithological unit than laboratory measurements mainly because well logs sample a finite volume of rock around the well and deliver an uninterrupted record with depth instead of sampling discrete point". "Despite well log being the best form of lithology and pore fluid prediction, uncertainties in measurements, complexities of geological formation, and many other factors result in unforeseen complications in lithology and pore fluid prediction" [6]. "In the past traditional well log interpretation techniques such as combining, and cross plotting of log data have been established using well logs data, and these methods are recently used for quick evaluations [6,7], but it has shortcomings where large heterogeneous reservoir data is concerned. Therefore to predict pore fluid and lithology of a large heterogeneous reservoir data several approaches such as petrophysics analysis and rock physics analysis have been presented" [8].

"Rock physics analysis establishes a bond between elastic rock properties (P–Impedance, S–Impedance, V_P/V_S ratio, rigidity modulus (μρ) and Incompressibility modulus (λρ), reservoir properties (lithology, water saturation, density, gamma ray, etc.), and architecture properties (fractures) [9] for lithology and pore fluid prediction. Rock physics is the study of rock types (lithology discrimination) and the types of fluid (fluid discrimination) in them" [10]. "In Niger Delta, the rock types are always sand-shale sequence and the fluid types are brine and hydrocarbon (oil and gas) which constitute the major fluids preserved in the Niger Delta reservoir basin" [10]. "Reservoirs are porous, permeable, well-sealed/trapped, and thick lithologic units that can harbour these fluids" [10, 11]. "The fluids which are majorly brine and hydrocarbon saturations usually occur in different proportions because the levels of saturation are not constant across reservoirs. It is not common to find a reservoir that is fully saturated with only gas or oil" [10].

According to [11], "rock properties and attributes were extracted using empirical rock physics models on well logs and were used to validate their potentials as pore fluid discriminants". "Then cross plotted to determine their sensitivity to fluid and lithology in cross plot space. Their identified depth for the reservoir of interest (A2) was in the range of 5842 ft to 5964 ft and 5795 ft to 5936 ft for Well A and B respectively. The properties cross plotted were Vp against Vs, Vp/Vs against Ip, Vp/Vs against Porosity, Vp/Vs against Density, and Vp against Density. The result of Vp against Density cross plot revealed that the reservoir consists of sand lithology with intercalated shale" [11]. "Vp against Vs shows a linear relationship and does not discriminate fluid in the reservoir. Vp/Vs ratio against Ip distinguishes reservoir of interest A2 into hydrocarbon, brine, and shale zones. Vp/Vs ratio against density and porosity cross-plots distinguishes the reservoir of interest A2 into gas, oil, brine, and shale zones" [11]. "Their analyses validate the fact that Vp/Vs ratio and their combinations cross plots are more sensitive and robust for fluid discrimination. It also reveals that

the ratio of Vp/Vs is more sensitive to the change of fluid type than the use of Vp or Vs separately" [11].

Okoli et al. [12] carried out "a cross-plot analysis of rock properties for gas detection in Soku Field, Coastal Swamp Depobelt, Niger Delta Basin using well data X-26 for a given oil field". "The study employed a rock physics algorithm on Hampson Russell software (HRS), rock attributes including V_p/V_s ratio, Lambda-Rho, and Mu-Rho was also extracted from the well data. Cross-plotting was carried out and Lambda Rho (λ_ρ) versus Mu-Rho (μ_ρ) cross-plots proved to be more robust for lithology identification than V_p versus V_s cross-plots, while λ_ρ versus Poisson Impedance was more robust than V_p/V_s versus Acoustic Impedance for fluid discrimination, as well as identification of gas sands" [13].

The aim of the study is to carry out fluid and lithology discrimination of HAX field, offshore, Niger Delta by (1) delineating reservoir sand bodies using well logs in the study area, (2) computing the elastic rock attributes such as Lame's parameters terms (λρ and μρ), Vp/Vs ratio, P-Impedance, and S-Impedance from available petrophysical data obtained from the well logs, (3) cross-plotting petrophysical and elastic rock attribute to delineate fluid and lithology in the reservoirs from well log, and (4) determine which attributes best discriminate fluid and lithology.

2. LOCATION OF THE STUDY AREA

The study area is located at HAX field, within the offshore area of Niger Delta in Nigeria (Fig. 1). The terrain is generally swampy, with river channels and tributaries emptying into the Atlantic Ocean. The field lies between longitude 7°31'34.2491"E and latitude 4°06'19.5656"N and is located within the central swamp depobelt, offshore Niger Delta.

3. GEOLOGY OF THE STUDY AREA

"The Niger Delta basin is situated at the southern end of Nigeria boarding the Atlantic Ocean and extends from about longitude 3^0E to 9^0E and latitude $4^0$3'N to $5^0$2'N" [14,15]. "Petroleum occurs throughout the Agbada formation of the Niger Delta. However, several directional trends form an oil-rich belt having the largest field and lowest gas-to-oil ratio" [16]. "The basin is an extensional rift basin located in the Niger Delta and the Gulf of Guinea on the passive continental margin near the Western coast of Nigeria with proven access to Cameroon, Equatorial Guinea, and Sao Tome and Principle" [17]. "It extends from the Calabar Flank and the Abakaliki Trough in Eastern Nigeria to the Benin Flank in the west and it opens to the Atlantic Ocean in the southern territory. The basin is very complex, and it carries high economic value as it contains a very productive

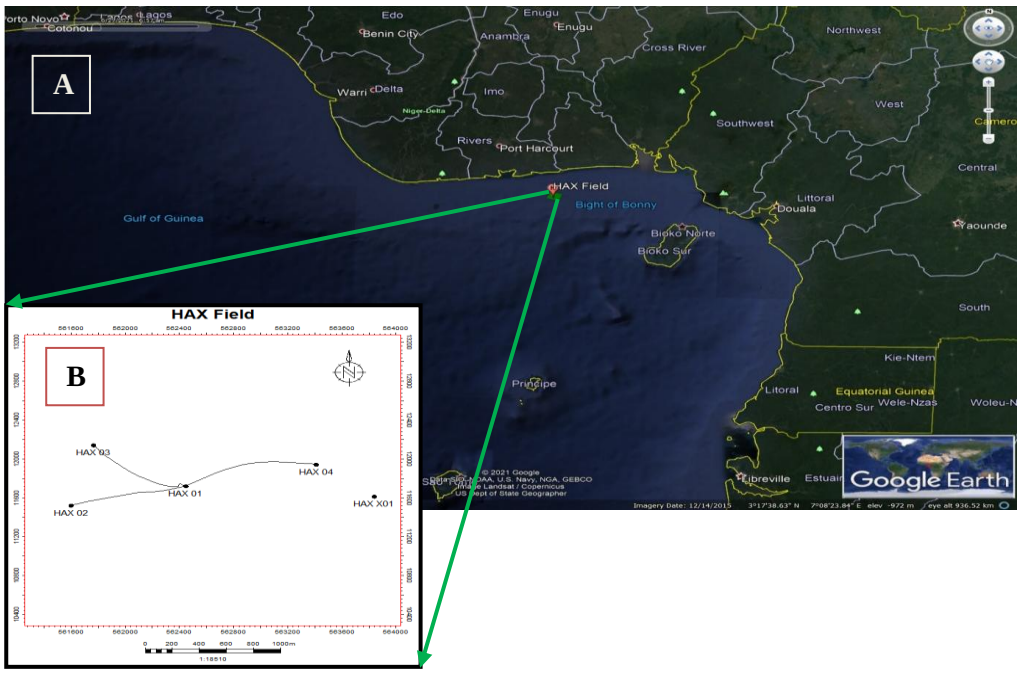

Fig. 1. (A) Location of the study area [13] and (B) the Base map for HAX Field

hydrocarbon system" [18]. "The Niger Delta basin is one of the largest subaerial basins in Africa. It has a subaerial area of about 75,000 km^2, a total area of 300,000 km^2, and a sediment fill of 500,000 $km^{3"}$ [18]. "The delta protrudes into the Gulf of Guinea as an extension from the Benue Trough and Anambra Basin Provinces" [19]. "The Niger Delta Basin is situated in the Gulf of Guinea and extends throughout the Niger Delta oil and gas province. From the Eocene to the present (Fig. 2), the delta has prograded southwestward, resulting in Depobelts that represent the most active portion of the delta" [16]. "The stratigraphy of the Niger Delta clastic wedge has been documented during oil exploration and production; most stratigraphic schemes remain proprietary to the major oil companies operating in the Niger Delta basin. The composite tertiary sequence of the Niger Delta consists of the Akata, Agbada and Benin formations" [17]. "These formations laid in an ascending order, and are composed of estimated 28,000 ft (8,535 m) section with approximate depocenter located in the central part of the delta" [20].

"The Akata Formation is the oldest and regarded as the primary source rock in the Niger Delta [21] which comprises marine shales, with few sandstone lenses, silt, and turbiditic sands with a 20% to 80% sand shale ratio" (Fig. 2). "The Eocene Agbada formation rests on the Paleocene Akata Formation composing the interbeddings of sands and shales that are paralic sedimentation" [22] (Fig. 2). [16] opined that "it is within this Agbada paralic section (Agbada Formation) that oil and gas exploitation occur in the Niger delta; with most of the traps being structural, developed due to synsedimentary deformation" [16].

The Agbada Formation consists of sandstone, alternation of sand-shale units in the delta. The sandstone units are major petroleum-bearing units that house the hydrocarbon" [23]."The formation has a thickness of about 4000 meters and represents the true deltaic portion of the sequence" [23]. "Agbada Formation is also called the parallic Agbada Formation because the shale and sandstone beds were deposited in equal proportions. Though, the upper part is mainly characterized by sand with minor shale interbeds" [23]. Agbada formation is composed of a 60% to 40% sand shale ratio. The last formation is the youngest in the Delta, the Oligocene Benin Formation, and rests conformably on the Eocene Agbada formation (Fig. 2). It has an average thickness of about 3050m and is composed of predominantly Continental River [24]. The Benin Formation's Top is composed mainly of alluvium and it is deposited in the alluvial or upper coastal plain environments.

4. MATERIALS AND METHODS

Well log data acquired from HAX field (HAX 01, HAX 02, HAX 03, and HAX 04), offshore Niger Delta (Table 1) comprises gamma ray (GR) logs, caliper logs, porosity logs (neutron, density, and sonic) and resistivity logs. Additionally, well header information and well survey deviation data were also acquired. The well deviation survey file contains valuable information such as the well depth in feet, true vertical depth (TVD) in feet, DX and DY in meters, latitude and longitude in meters, inclination, azimuth, and X, Y, and Z coordinates all in degrees. This information will be helpful in analyzing and interpreting the well log data. It is important to note that all four wells from the HAX field deviate, meaning that they are not vertical but have some inclination and deviation from the vertical. This can have significant implications for the interpretation of the well log data and were taken into account during the analysis.

4.1 Software

Industry-based software utilized to carry out the analysis of the HAX field is Schlumberger PETREL™ (2017 version) Software (used for loading well log data, data appraisal, well correlation, and petrophysical data analysis) and RokDoc 6.6.1.133 Software (used for loading, cross-plotting, visualizing and analyzing elastic log properties estimated).

4.2 Methods

The following outlined procedures and workflow (Fig. 3) was carried out for the successful completion of this study. This procedure includes data sourcing, data loading into relevant software, data quality assurance and quality control, well logs conditioning (despiking and interpolation), well correlation, petrophysical evaluation of reservoirs, visualization, analysis of estimated petrophysical properties, estimation of elastic log properties, cross-plot, and analysis of the rock elastic log properties.

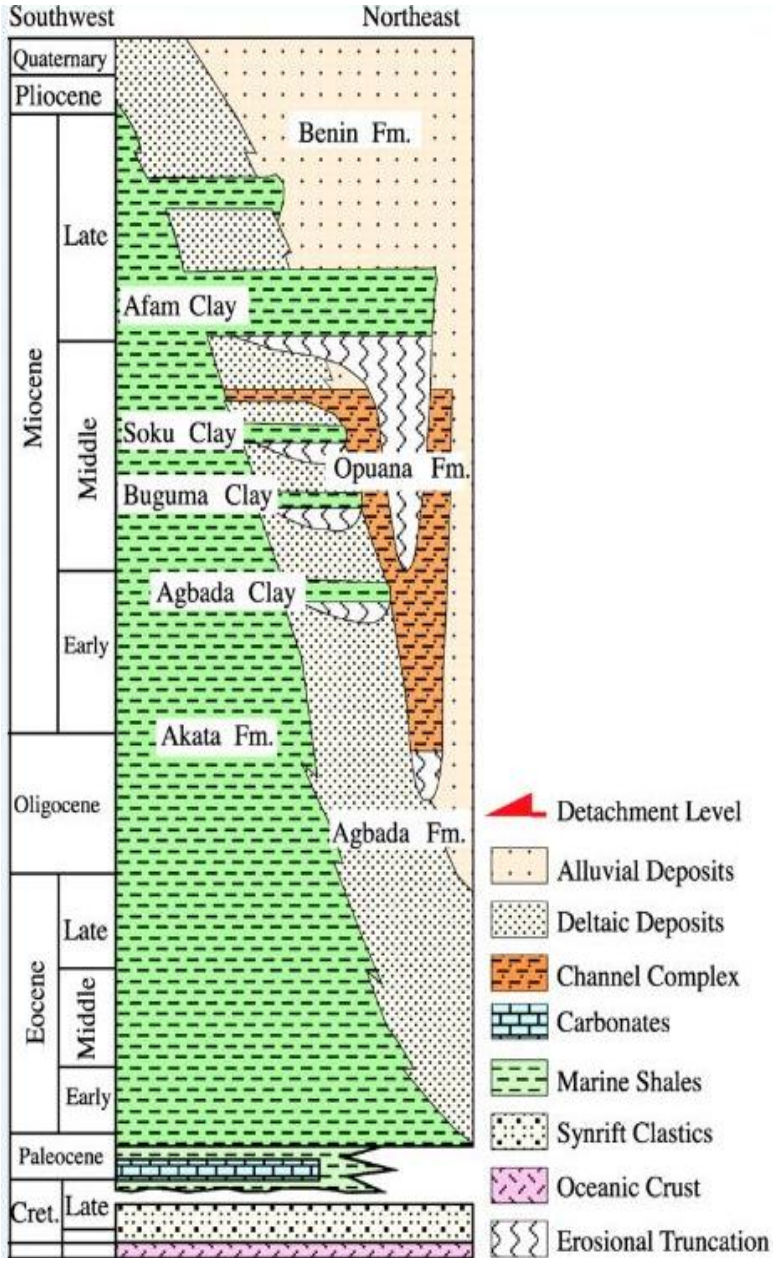

Fig. 2. Regional Stratigraphy of the Niger Delta [25,26]

4.3 Data Import and Quality Check

Well Information which, include well header, well deviation survey, and well log parameter was imported into the industry-based software and cross-checked for errors in the data before proper analysis of the well data began, this was done using the two software.

Table 1. Suite of Logs in each Well.(Y=YES, N=NO)

Wells	Available logs							
	GR	RT	RHOB	NPHI	DT	CALI	SP	CS
HAX 01	Y	Y	Y	Y	Y	Y	Y	Y
HAX 02	Y	Y	Y	Y	Y	Y	Y	Y
HAX 03	Y	Y	Y	Y	Y	Y	Y	N
HAX 04	Y	Y	Y	Y	Y	Y	N	Y

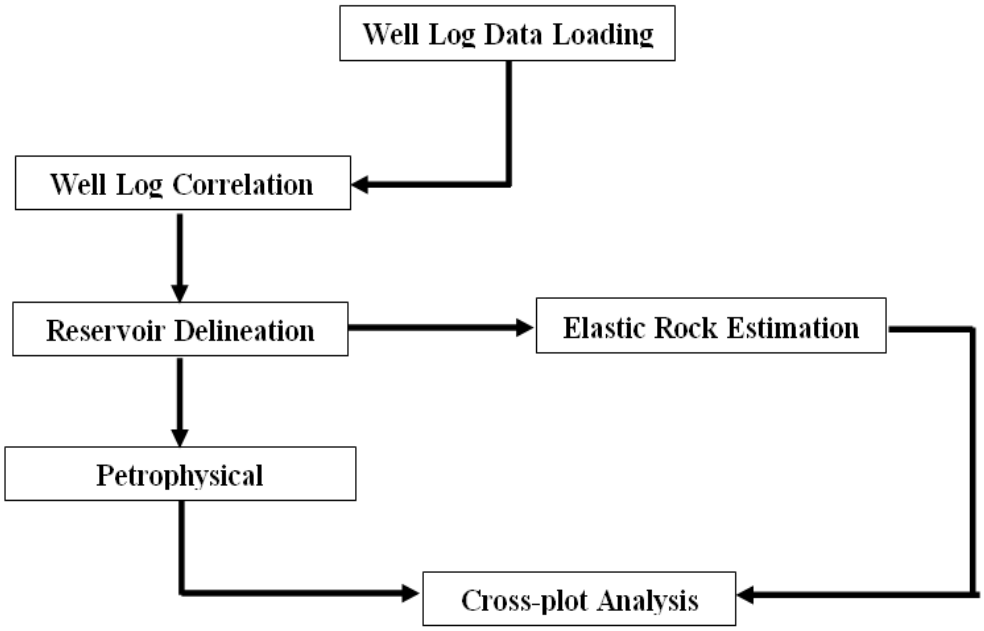

Fig. 3. Workflow adopted for HAX Field study analysis

Table 2. Elastic attributes and their empirical formulas

Elastic rock properties	Empirical formulas
Acoustic Impedance (P–Impedance)	$V_P * \rho$
Shear Impedance (S–Impedance)	$V_S * \rho$
V_P/V_S ratio	$\frac{V_P}{V_S}$
Mu	ρV_S^2
Mu-Rho ($\mu\rho$) Mu-Rho was defined as the multiplication of rock density and rigidity	$\rho(\rho V_S^2)$ $(\rho V_S)^2$
Lame's Lambda constant (λ) The measure of the fluid's ability to resist compression, hence it is sensitive to pore fluid and sometimes called fluid incompressibility	$\rho(V_P^2 - 2V_S^2)$
Lambda-Rho Where c is the discriminator factor ranging from "2.00 to 2.233" for robust discrimination of fluid and lithology [29], "I_S" and "I_P" are S-wave and P-wave Impedances, respectively [30].	$\lambda\rho = (\rho V_P)^2 - 2(\rho V_S)^2$ $\lambda\rho = I_P^2 - 2I_S^2$ $\lambda\rho = I_P^2 - cI_S^2$

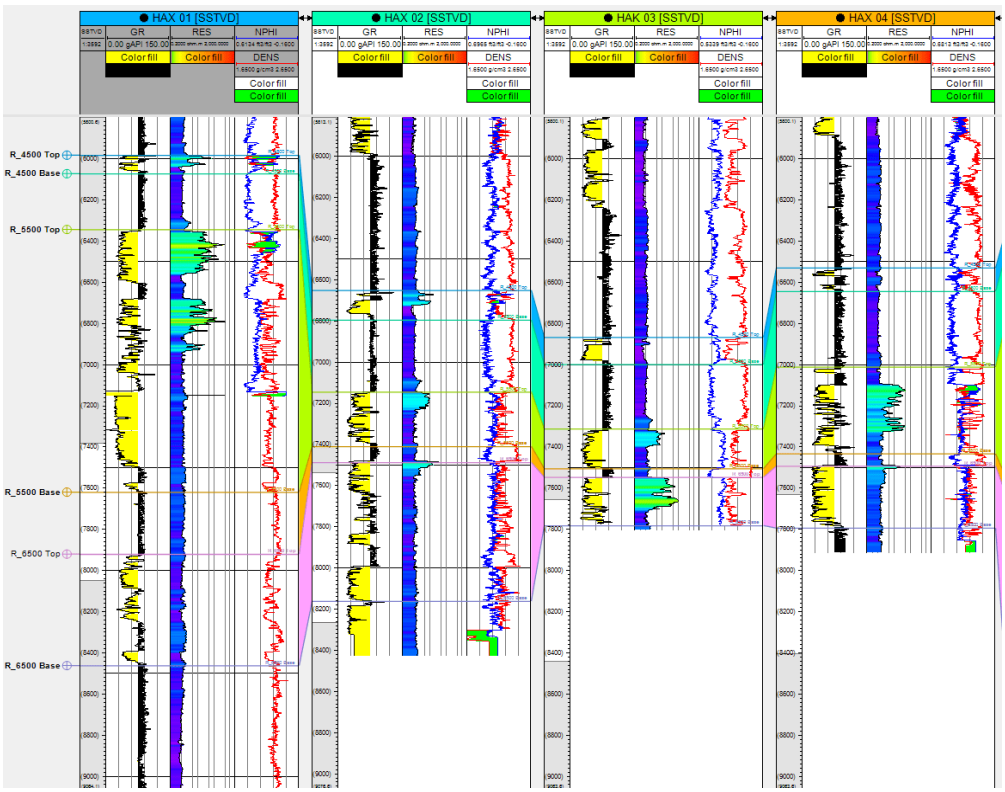

Fig. 4. Well Correlation in HAX Field across the four well

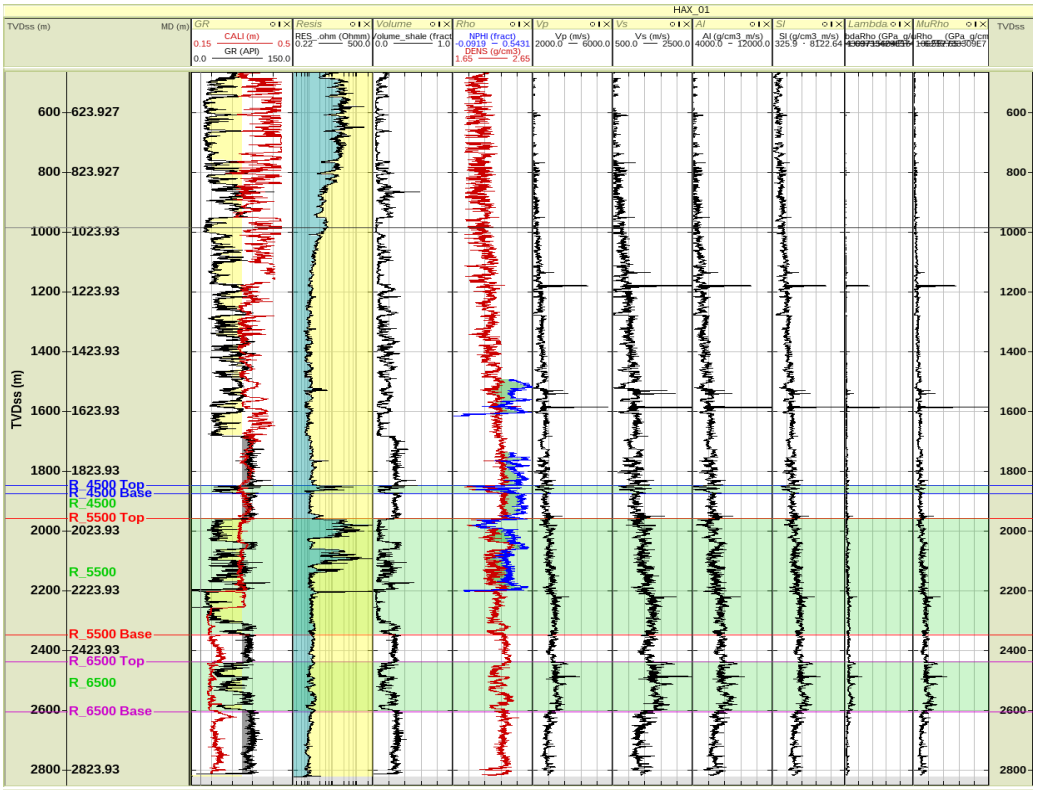

Fig. 5. Elastic rock properties estimated from HAX 01

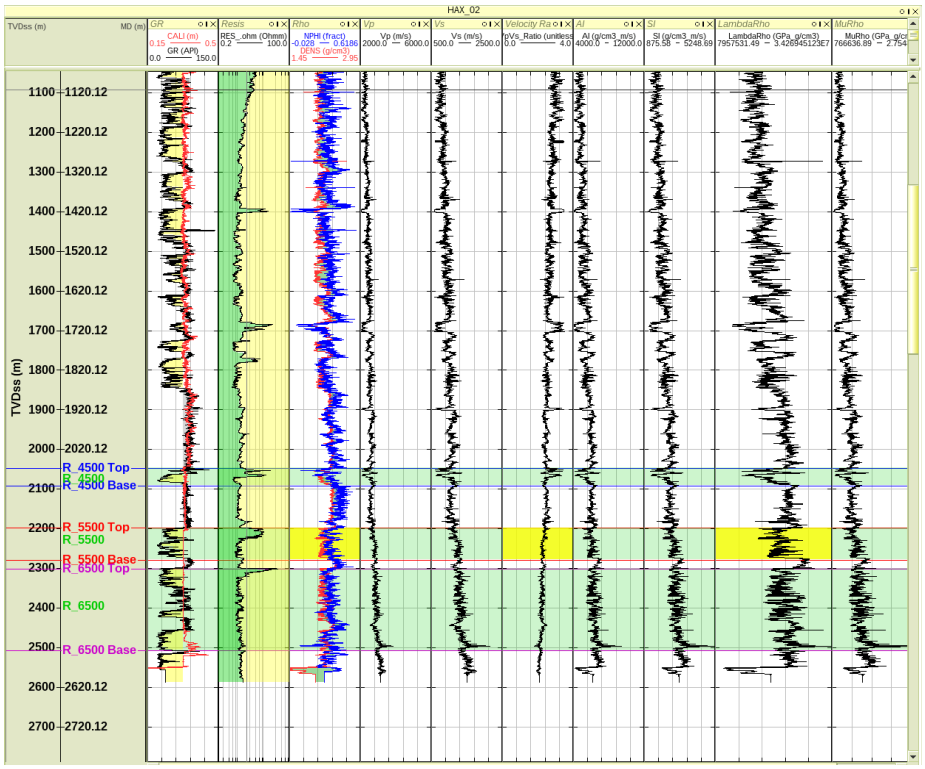

Fig. 6. Elastic rock properties estimated from HAX 02

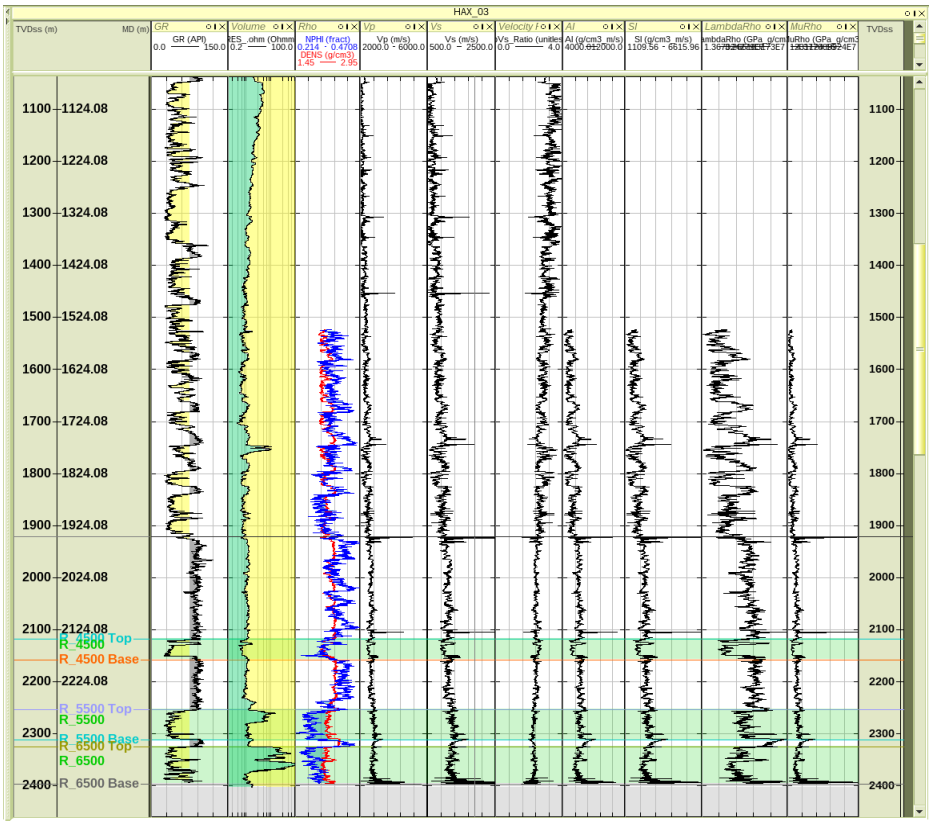

Fig. 7. Elastic rock properties estimated from HAX 03

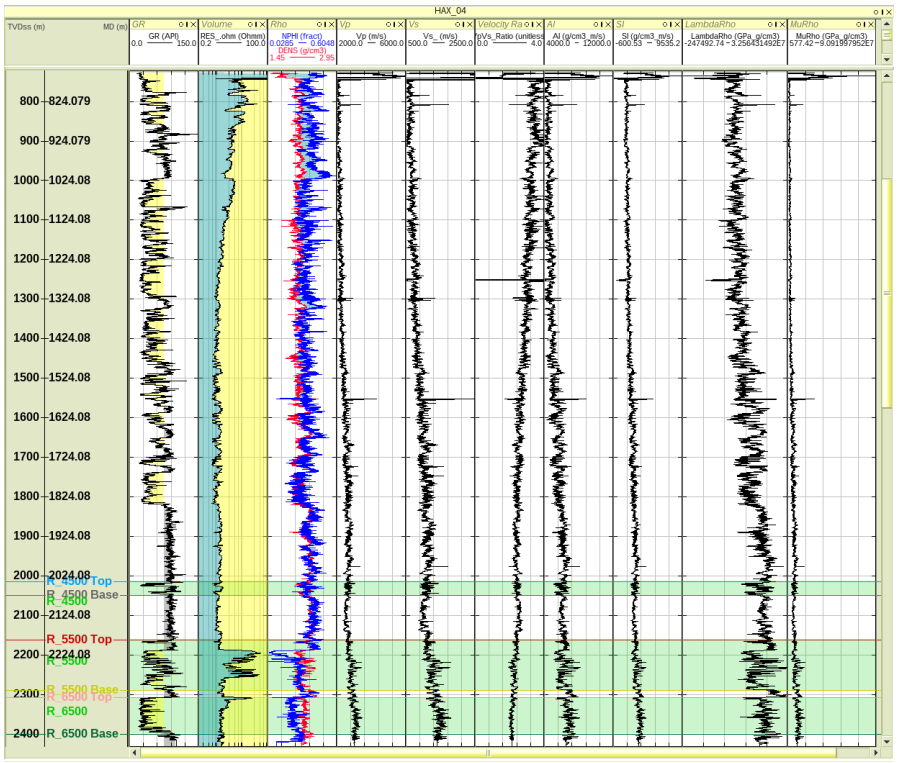

Fig. 8. Elastic rock properties estimated from HAX 04

4.4 Water Saturation Estimation

Archie's empirical equation [27] was utilized for water saturation (*S*w), which is simply the proportion within the total reservoir pore volume occupied by formation water.

$$\mathrm{Sw} = \left(\frac{a \times R_w}{R_t \times \emptyset_t^m}\right)^{1/n} \quad (1)$$

Where;

S_w = Archie's water saturation for clean sand
a = Tortuosity factor that is 1
m = Cementation exponent which is 2
n = Saturation exponent that is 2
Rt = Formation resistivity (read from log)
Rw = Formation water resistivity (read from log)
Φ_t = Total Porosity

4.5 Elastic Rock Property Estimation

To generate the rock physics attribute S-wave velocity was first derived using the empirical formula given by Castagna's mud rock line equation [28].

$$V_P = 1.16V_S + 1360\,ms^{-1} \quad (2)$$

Thereafter, P–Impedance, S–Impedance, V_P/V_S ratio, rigidity modulus (μρ), and Incompressibility modulus (λρ) were transformed from existing P-wave velocity, derived S-wave velocity, and density logs (Table 2). Cross plots were then carried out for the discrimination of fluid and lithology using the well log data.

5. RESULTS AND DISCUSSION

Cross-plots are graphical representations of the correlation between two or more independent variables that are used to visually identify or identify anomalies that could be interpreted as the existence of hydrocarbons or other fluids and lithologies [13]. In this study, the cross plots of the following were carried out;

1. Lambda-Rho against V_P/V_S ratio
2. V_P/V_S ratio versus P-Impedance
3. Mu-Rho against Rho
4. Lambda-Rho against Mu-Rho

They were color coded with attributes such as gamma ray, density, resistivity, and water saturation to successfully distinguished between fluids and lithology. The reservoir properties were found to have a linear relationship. The observed

results correspond with findings made by Alabi and Enikanselu [31].

5.1 Lambda-Rho against V_P/V_S Ratio

Figs. 9-11 show the variation of lambda-rho (incompressibility) against Vp/Vs ratio for sand and shale sequences colour-coded by water saturation, gamma ray and density respectively. The cross-plot in Figs 9(A-D) shows the shale zone described black ellipse, the blue describes brine sand, and the orange ellipse describes hydrocarbon sand zone using water saturation (Sw) as colour indicator. Using gamma ray (GR) as colour-code in Figs. 10(A-D), the plots are simply differentiated into sand and shale sequence with the blue ellipse indicating the shale zone and the orange ellipse indicating the

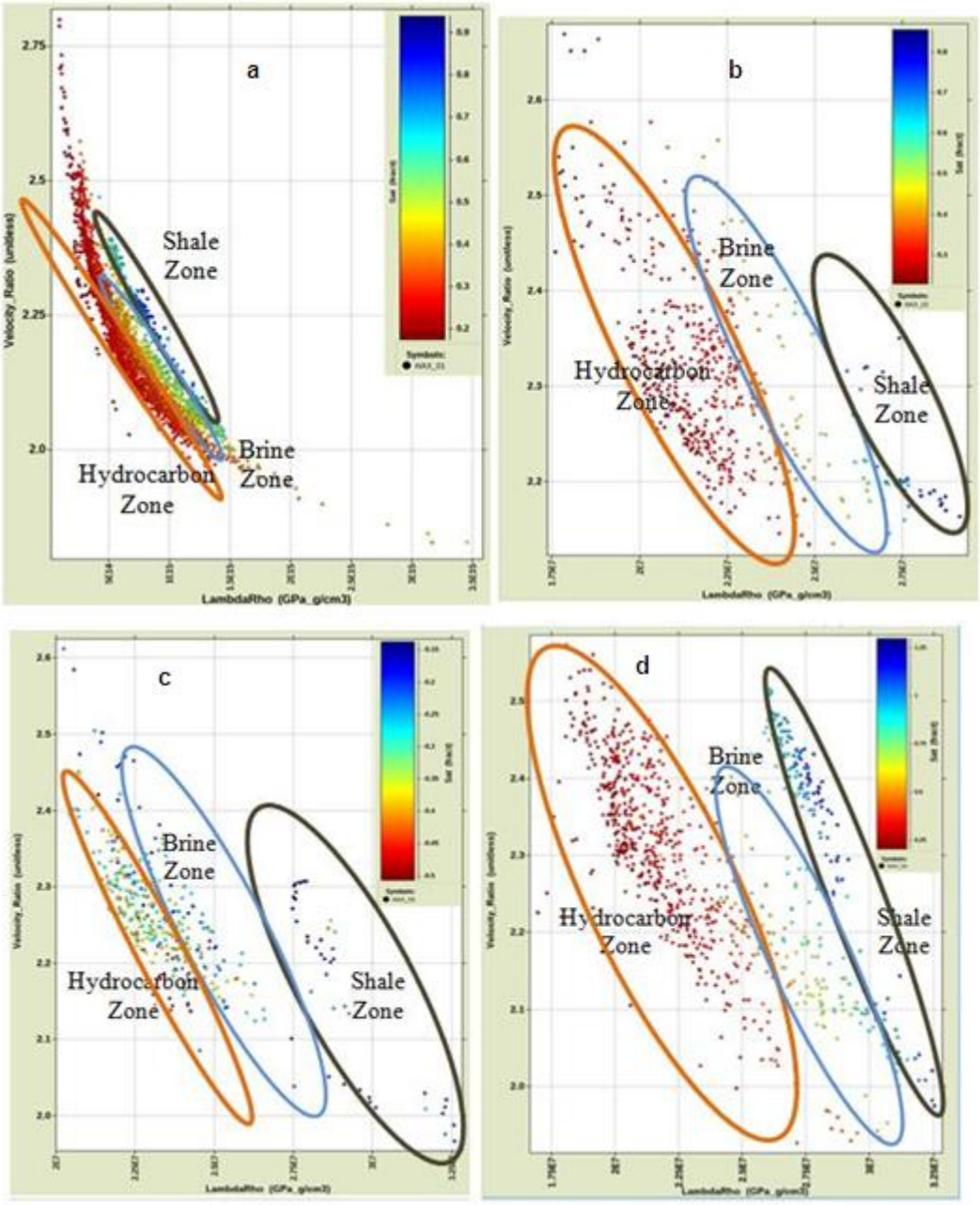

Fig. 9. Cross plot of Lambda-Rho (λρ) versus V_P/V_S ratio color coded with Water Saturation for (a) HAX 01 (b) HAX 02 (c) HAX 03 (d) HAX 04

sand zone. For the density colour indicator in Fig. 11(A-D), the black ellipse reveals the shale zone, ellipse the brine sand zone, the orange ellipse the oil zones and the purple ellipse the gas zones.

5.2 V_P/V_S Ratio versus P-Impedance

Figs. 12-14 show the variation of the Vp/Vs ratio against Acoustic Impedance cross-plots colour-coded by water saturation, gamma ray, and density respectively. Fig. 12 (A-D) distinguishes the reservoir of interest into three zones namely; shale zone (black ellipse), brine sand zone (blue ellipse) and hydrocarbon sand zone (orange ellipse) colour-coded by Sw. Using gamma ray (GR) as colour-code in Figs. 13(A-D), the plots are simply differentiated into sand and shale sequence with the blue ellipse indicating the shale zone and the orange ellipse indicating the sand zone. For the density colour indicator in Fig. 14(A-D) distinguishes the reservoir of interest into four zones namely; shale zone (black ellipse), brine sand (blue ellipse), oil (orange ellipse) and gas sands (purple ellipse). The Vp/Vs ratio is lower in hydrocarbon bearing sand than shale since shear waves cannot propagate during fluids [32,33]. The results show shale having high values in each Vp/Vs and AI than hydrocarbon bearing sand with low values of AI and Vp/Vs ratio [32-36].

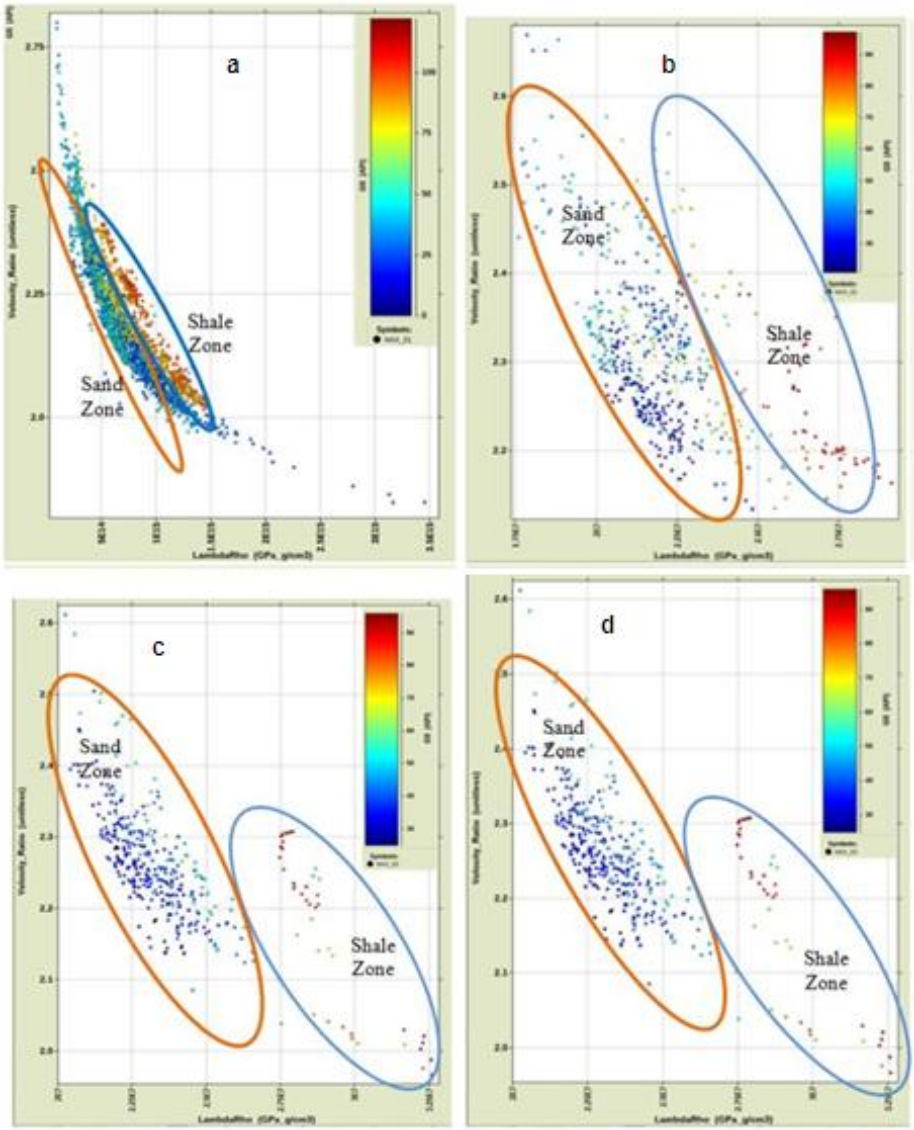

Fig. 10. Cross plot of Lambda-Rho (λρ) versus V_P/V_S ratio color coded with Gamma Ray for (a) HAX 01 (b) HAX 02 (c) HAX 03 (d) HAX 04

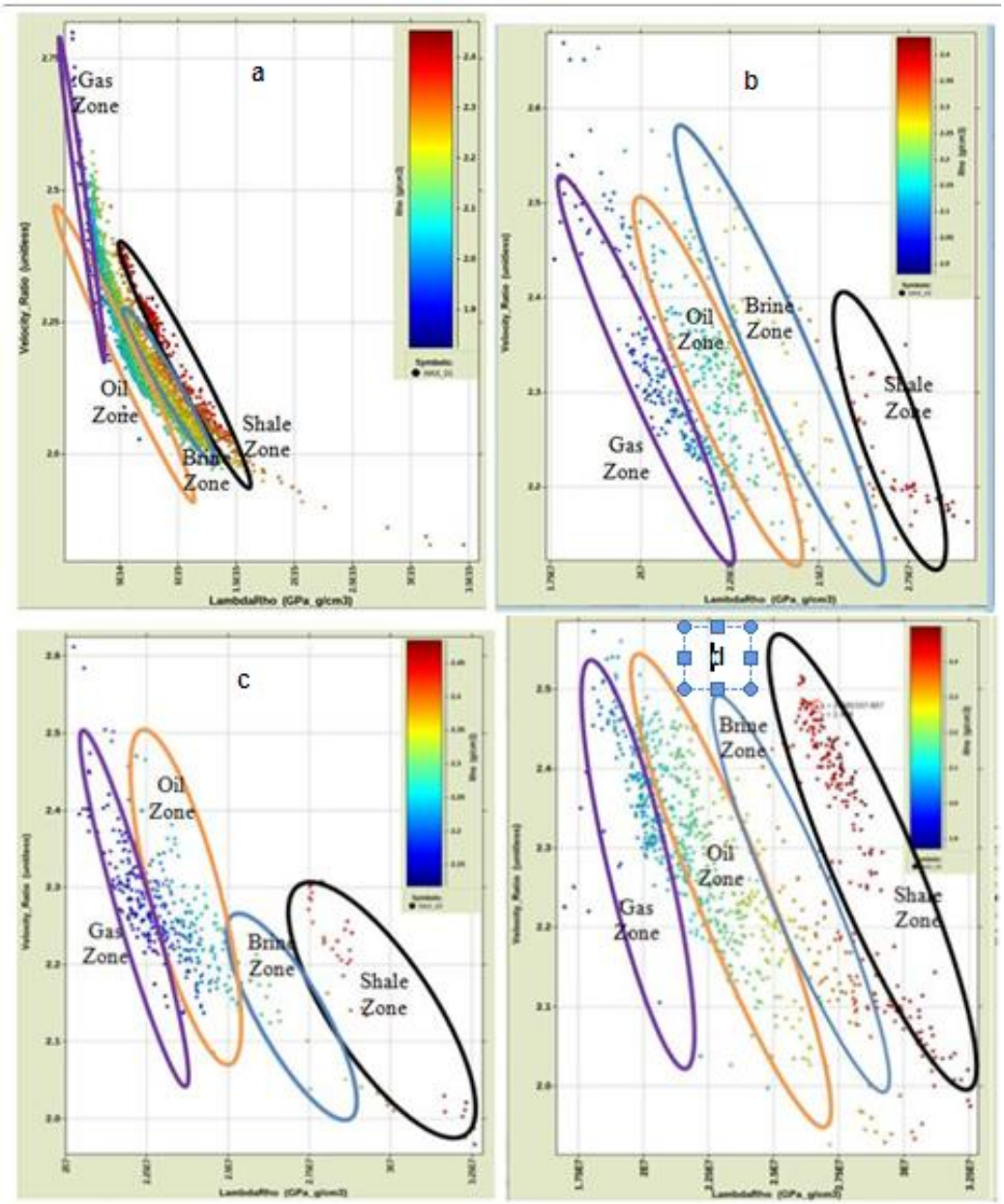

Fig. 11. Cross plot of Lambda-Rho (λρ) versus V_P/V_S ratio color coded with Density for (a) HAX 01 (b) HAX 02 (c) HAX 03 (d) HAX 04

The results also show that the hydrocarbon bearing sand density colour-code is lower than water saturated sand for hydrocarbon bearing sand because water is denser than oil while water saturated sand has a lower density than shale [36,37]. Therefore, clusters with higher density values coloured black represent shale, while the low density clusters coloured (orange and purple) represent hydrocarbon bearing [32-37].

This cross-plot shows better lithology and fluid discrimination along the acoustic impedance axis, indicating that the acoustic impedance attribute will better describe the R_5500 reservoir conditions in terms of lithology and fluid content than Vp/Vs ratio.

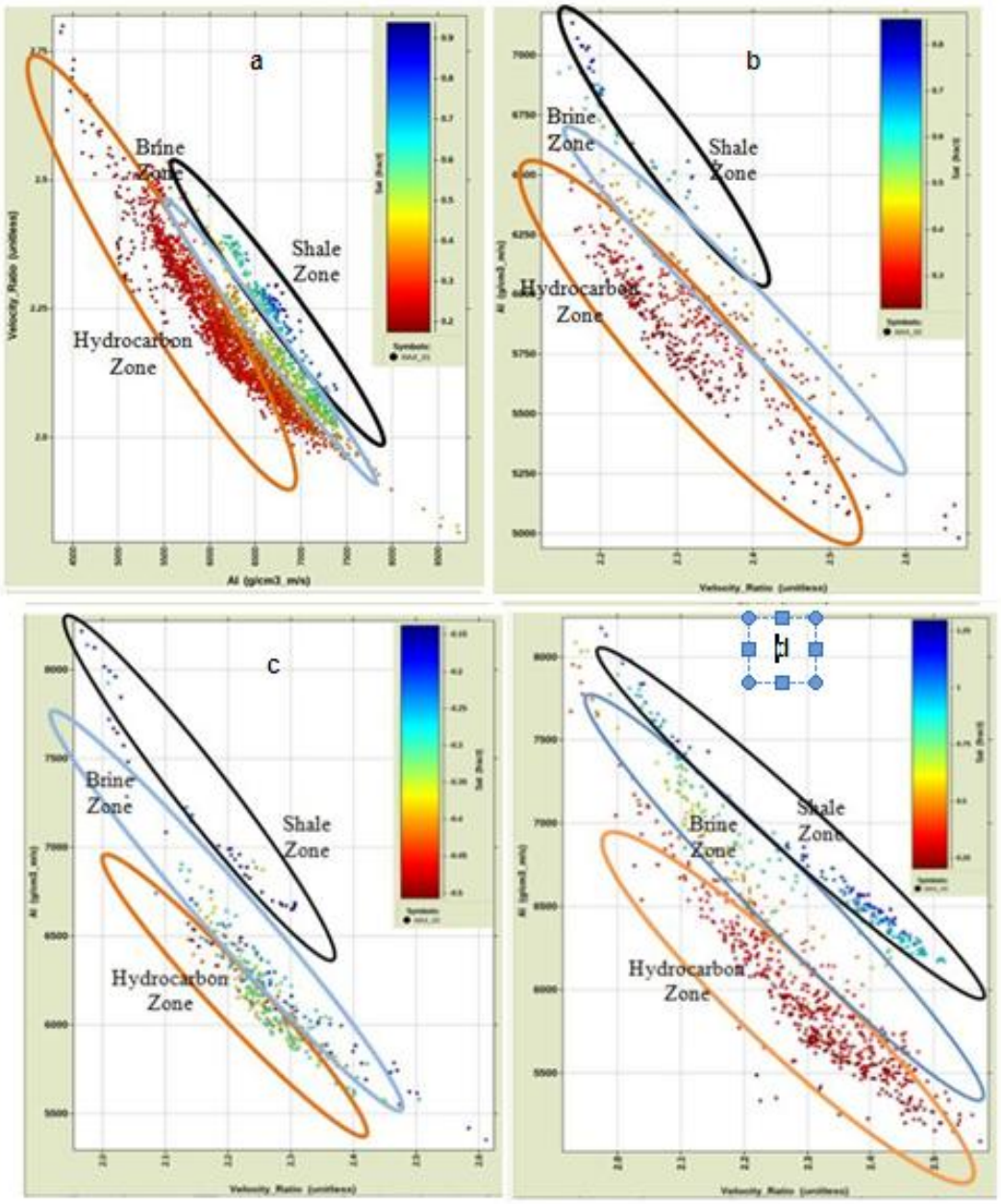

Fig. 12. Cross plot of V_P/V_S ratio against Acoustic Impedance color coded with Water Saturation for (a) HAX 01 (b) HAX 02 (c) HAX 03 (d) HAX 04

5.3 Mu-Rho against Rho

Figs. 15-17 show the variation of Mu-Rho against Density colour-coded by water saturation, gamma ray, and density respectively. In Fig. 15(A-D), the black ellipse describes the shale region, the blue ellipse describes brine saturated sand region, and the orange ellipse describes hydrocarbon bearing sand using water saturation (Sw) as a colour indicator. Using gamma ray (GR) as colour-code in Fig. 16(A-D), the plots are simply differentiated into sand and shale sequence with the blue ellipse indicating the shale zone and the orange ellipse indicating the hydrocarbon bearing sand. For the density colour indicator in Fig. 17(A-B), the cross-plot indicates that the black ellipse reveals the shale zone, the blue ellipse the brine sand, the orange ellipse the oil sand, and the purple ellipse the gas sand. Mu-rho and density are both lithology discriminators but density can also be used for fluid prediction, this is one of the advantages of density over Mu-Rho has seen from the cross-plots [33].

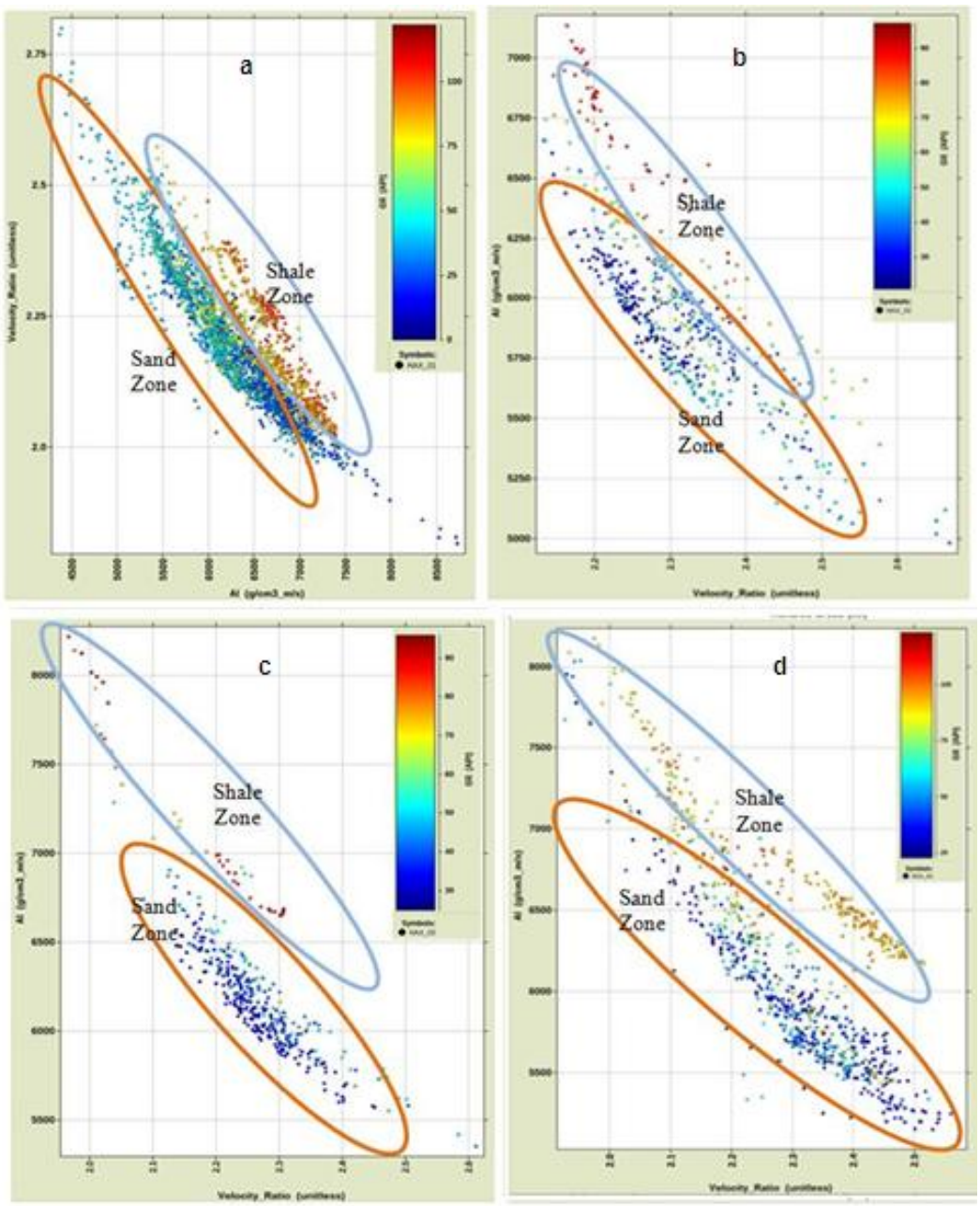

Fig. 13. Cross plot of V_P/V_S ratio against Acoustic Impedance color coded with Gamma Ray for (a) HAX 01 (b) HAX 02 (c) HAX 03 (d) HAX 04

In theory, sand will have a high value of Mu-Rho and a low value of shale [38] but in this field, the results of the cross-plots show that the Mu-Rho values are high for shale and low for sand while the density of shale is higher than that of sand [2,33]. Furthermore, hydrocarbon bearing sand is less dense than brine (even as hydrocarbon gas is less dense than oil) and brine is less dense than shale [2,33].

5.4 Lambda-Rho against Mu-Rho

Figs. 18-20 show the variation of Lambda-Rho (λρ) against Mu-Rho (μρ) colour-coded by water saturation, gamma ray, and density respectively.

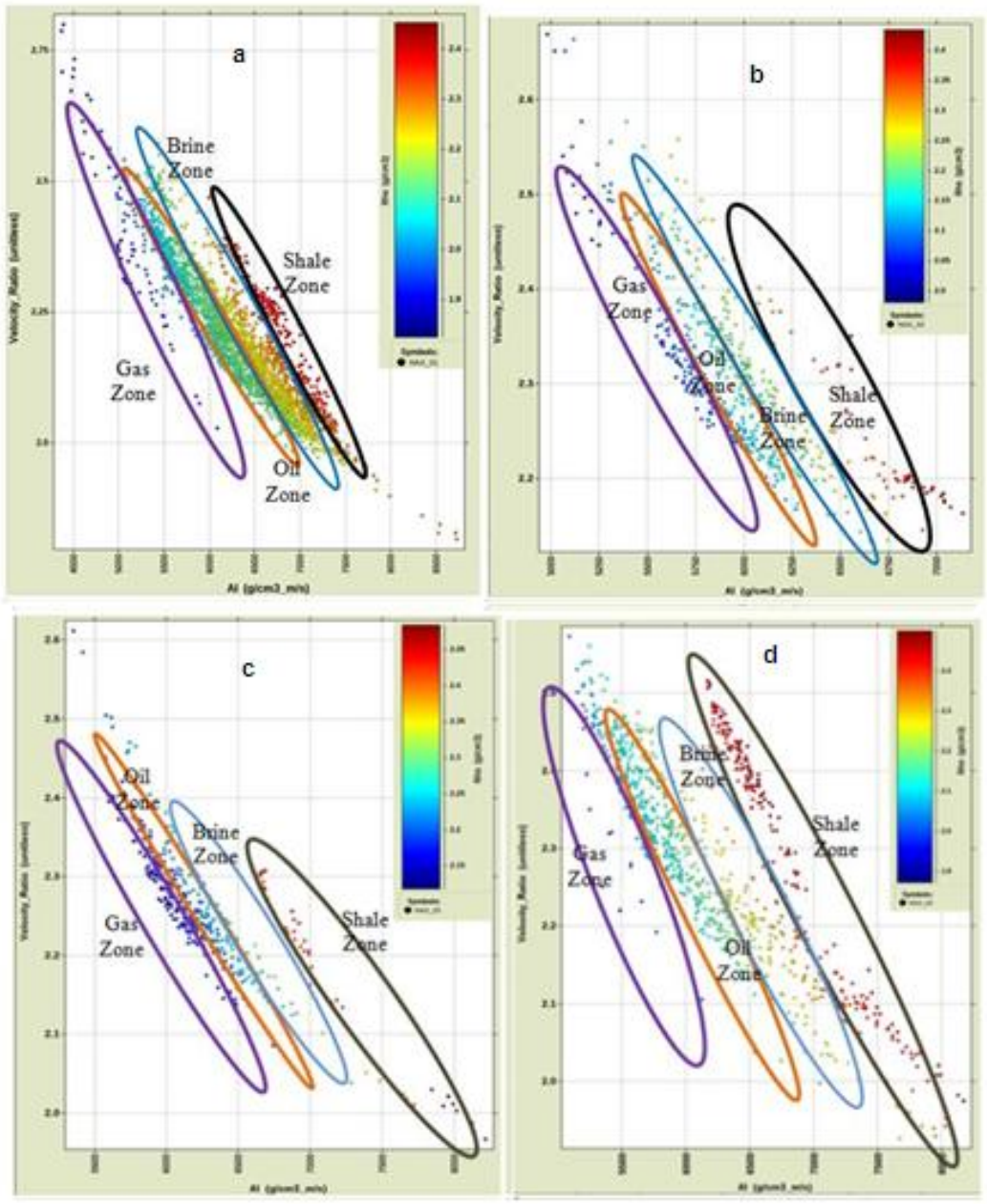

Fig. 14. Cross plot of V_P/V_S ratio against Acoustic Impedance color coded with Density for (a) HAX 01 (b) HAX 02 (c) HAX 03 (d) HAX 04

Fig. 18(A-D) the cross-plots are separated into three zones that can be inferred to be probable brine (black ellipse), oil (blue ellipse), and hydrocarbon bearing sand (orange ellipse) using water saturation (Sw) as colour indicator. Using gamma ray (GR) as colour, the plots are simply differentiated into sand and shale sequence with the blue ellipse indicating the shale zone and the orange ellipse indicating the hydrocarbon bearing sand (Fig. 19(A-D)). For the density colour indicator, the cross-plot reveals shale (black ellipse), brine (blue ellipse), oil (orange ellipse), and gas (purple ellipse). Brine (blue eclipse), oil (orange eclipse), and gas zone (purple eclipse) were confirmed by the lowest water saturation values (Fig. 20(A-D)).

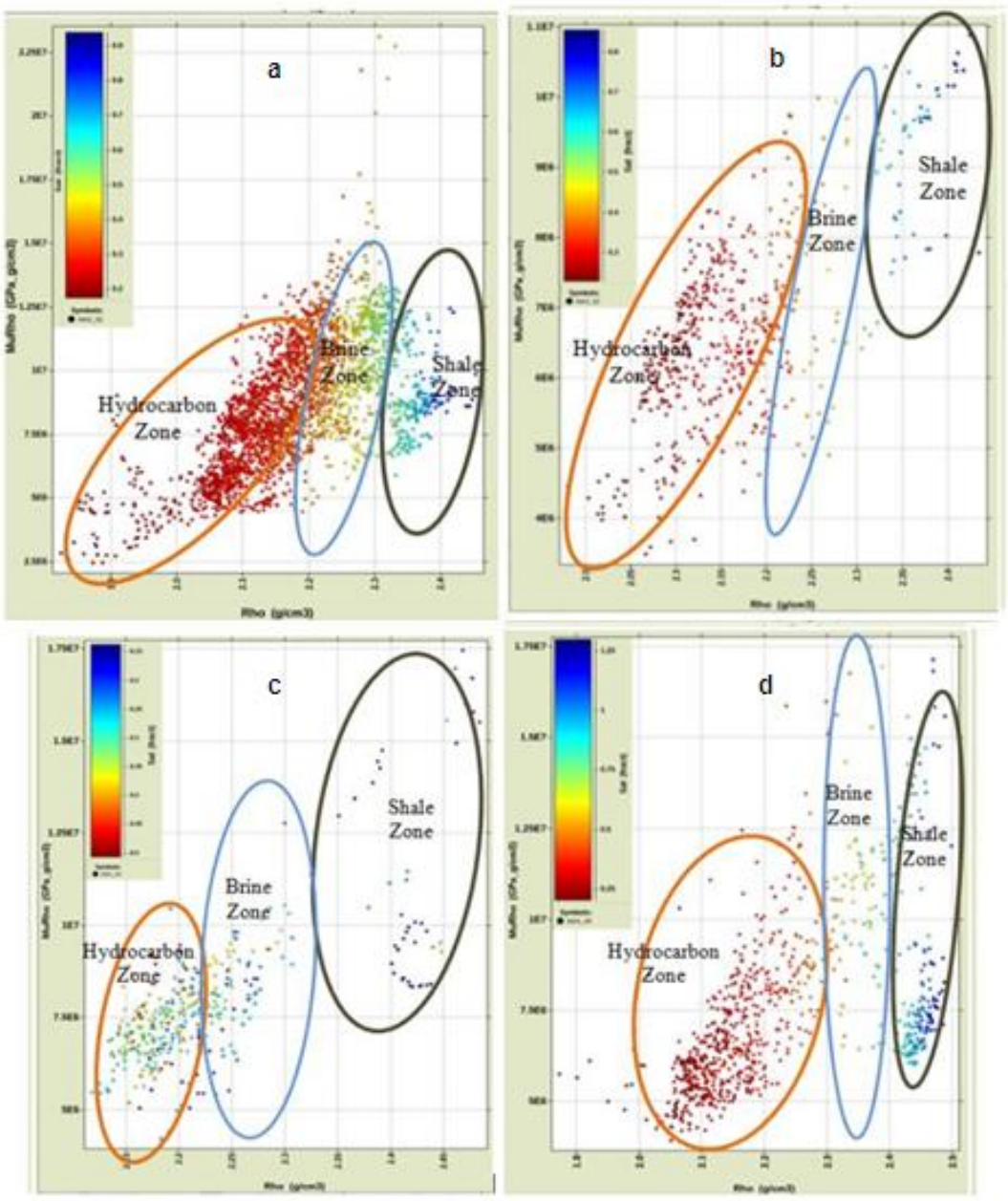

Fig. 15. Cross plot of Mu-Rho against density color coded with Water Saturation for (a) HAX 01 (b) HAX 02 (c) HAX 03 (d) HAX 04

The results show that the clusters were better separated from the background trend which falls within the reservoir region by Lambda- Rho more than Mu-Rho as in [10]. This makes Lambda-Rho a better fluid indicator than Mu-Rho which is a matrix indicator that helps to provide direct geological meaningful information about reservoirs [10]. The hydrocarbon zone showed the gas zone lower in Lambda-Rho and density responses than the oil zone [2,10,39-41]. The plot indicates that λρ is more robust than μρ in the analysis of fluids in the field of study and that μρ values are relatively low for the reservoir sand according to [2,3,10].

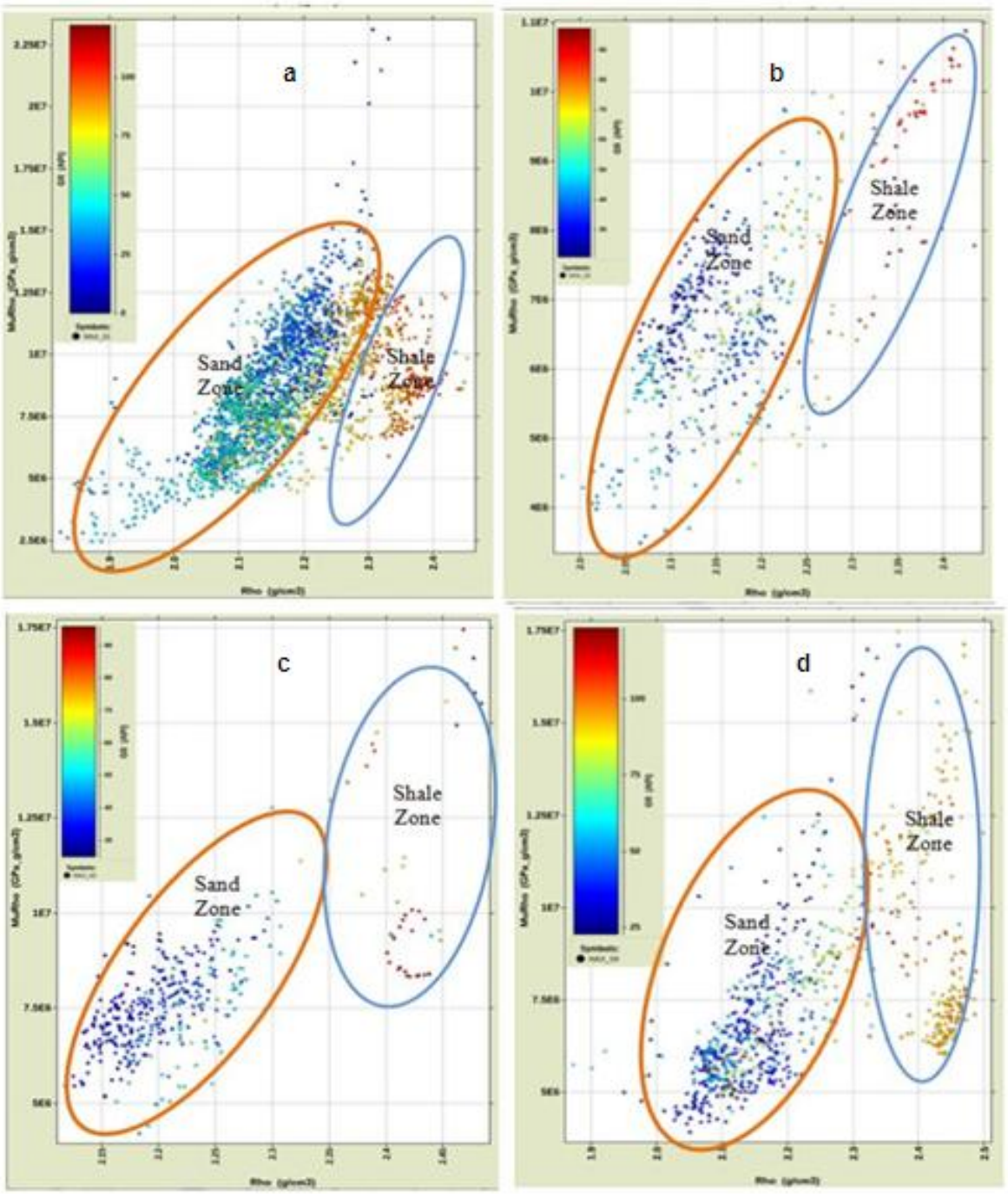

Fig. 16. Cross plot of Mu-Rho against density color coded with Gamma Ray for (a) HAX 01 (b) HAX 02 (c) HAX 03 (d) HAX 04

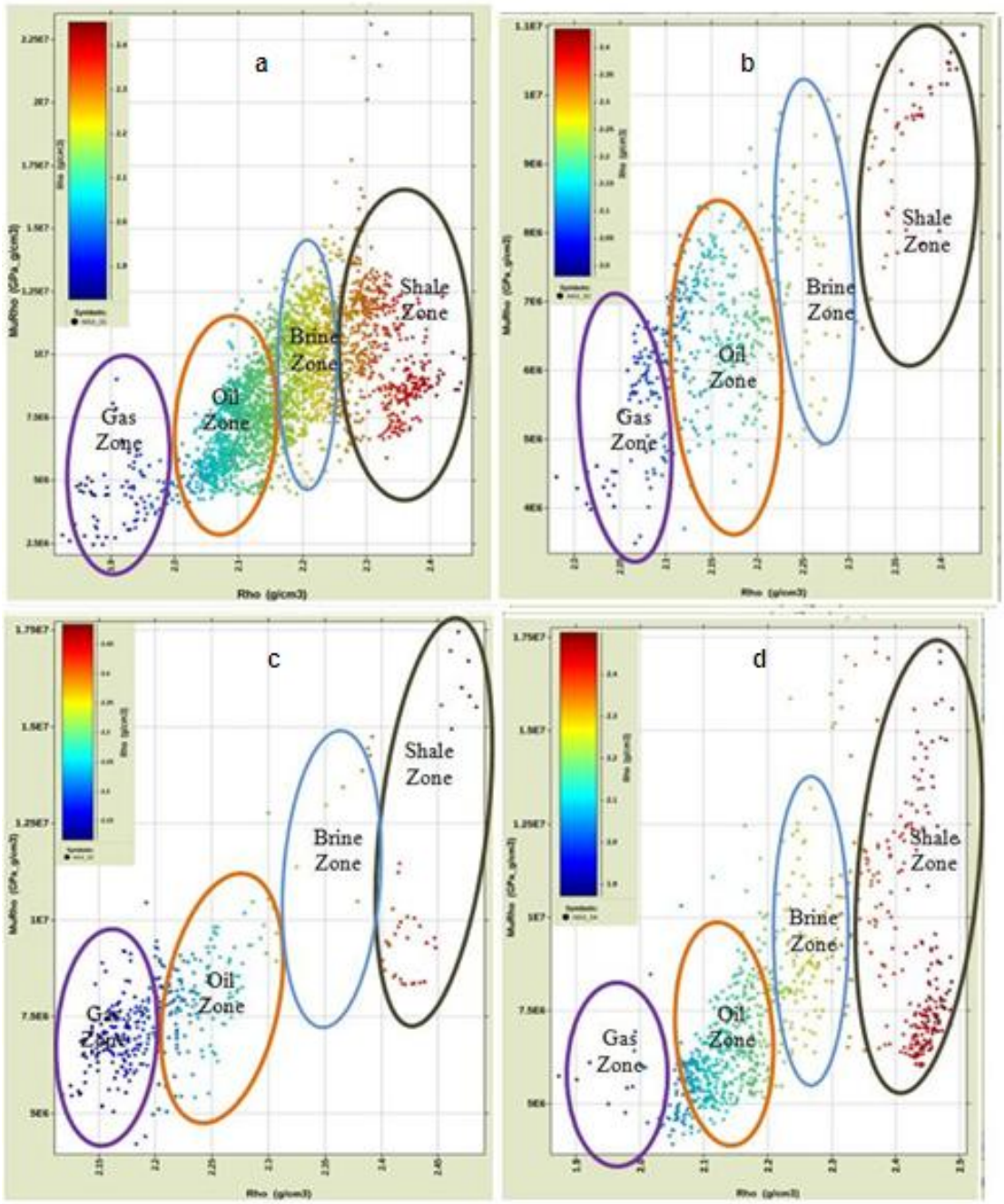

Fig. 17. Cross plot of Mu-Rho against density color coded with Density for (a) HAX 01 (b) HAX 02 (c) HAX 03 (d) HAX 04

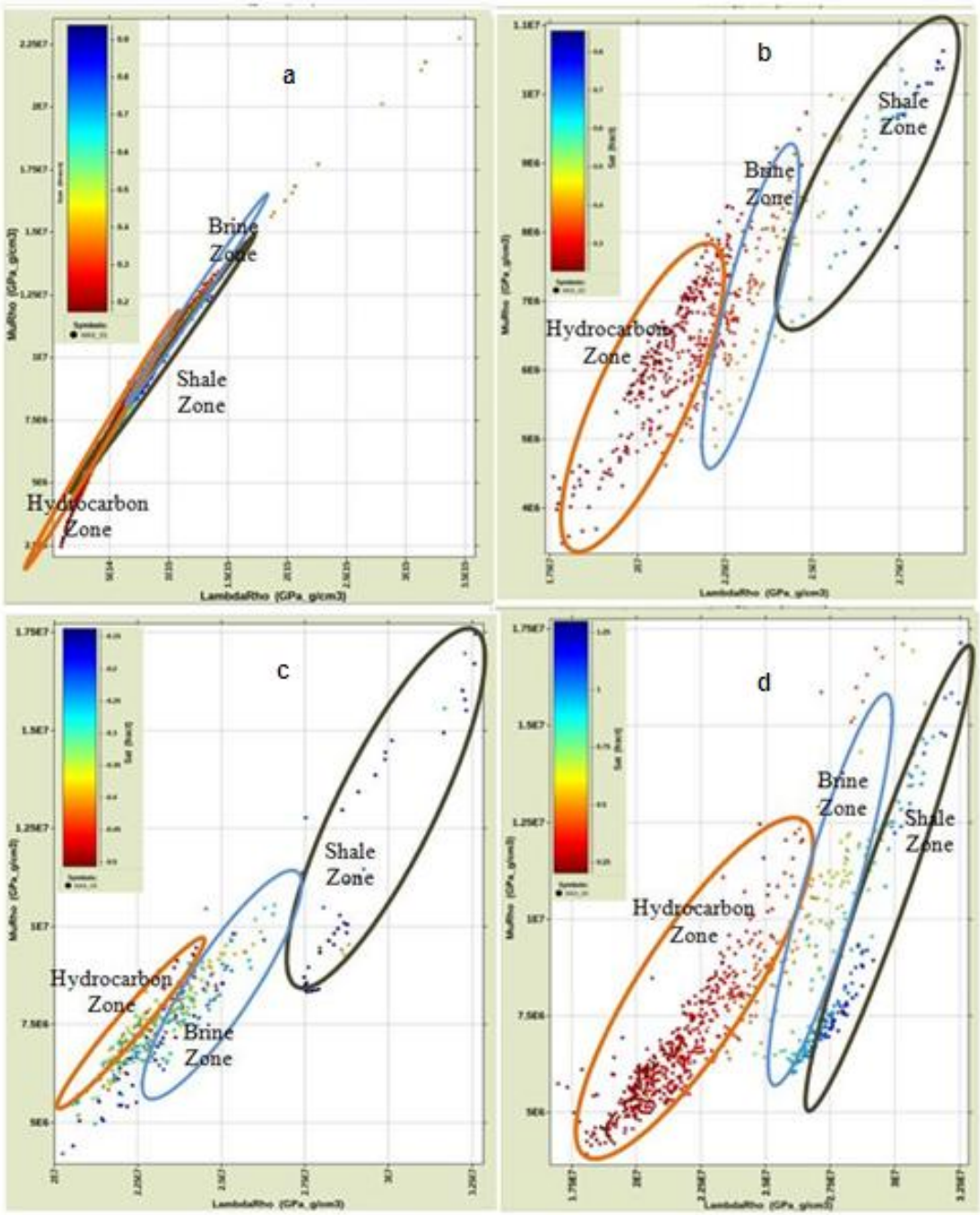

Fig. 18. Cross plot of Lambda-Rho (λρ) against Mu-Rho (μρ) color coded with Water Saturation for (a) HAX 01 (b) HAX 02 (c) HAX 03 (d) HAX 04

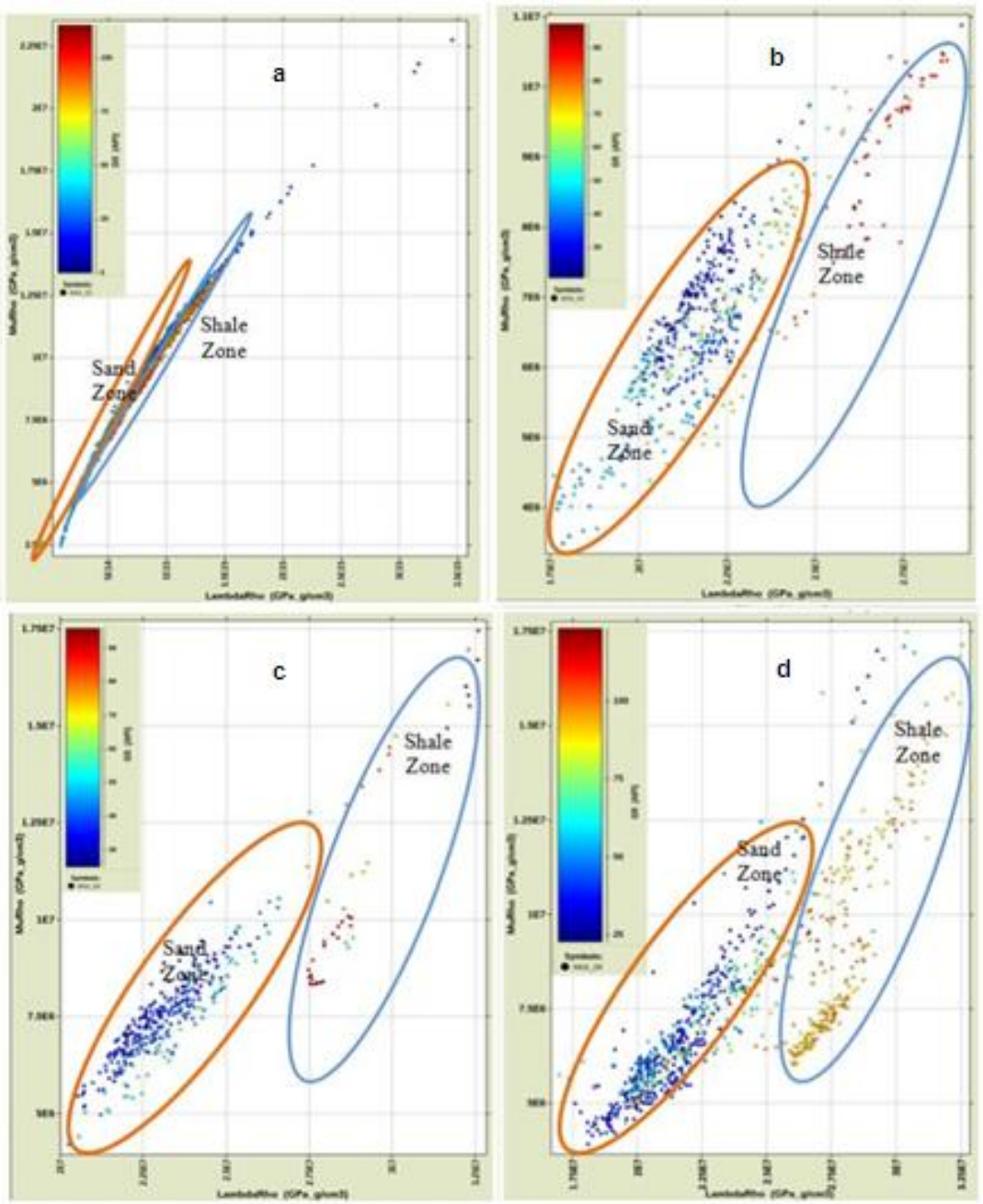

Fig. 19. Cross plot of Lambda-Rho (λρ) against Mu-Rho (μρ) color coded with Gamma Ray for (a) HAX 01 (b) HAX 02 (c) HAX 03 (d) HAX 04

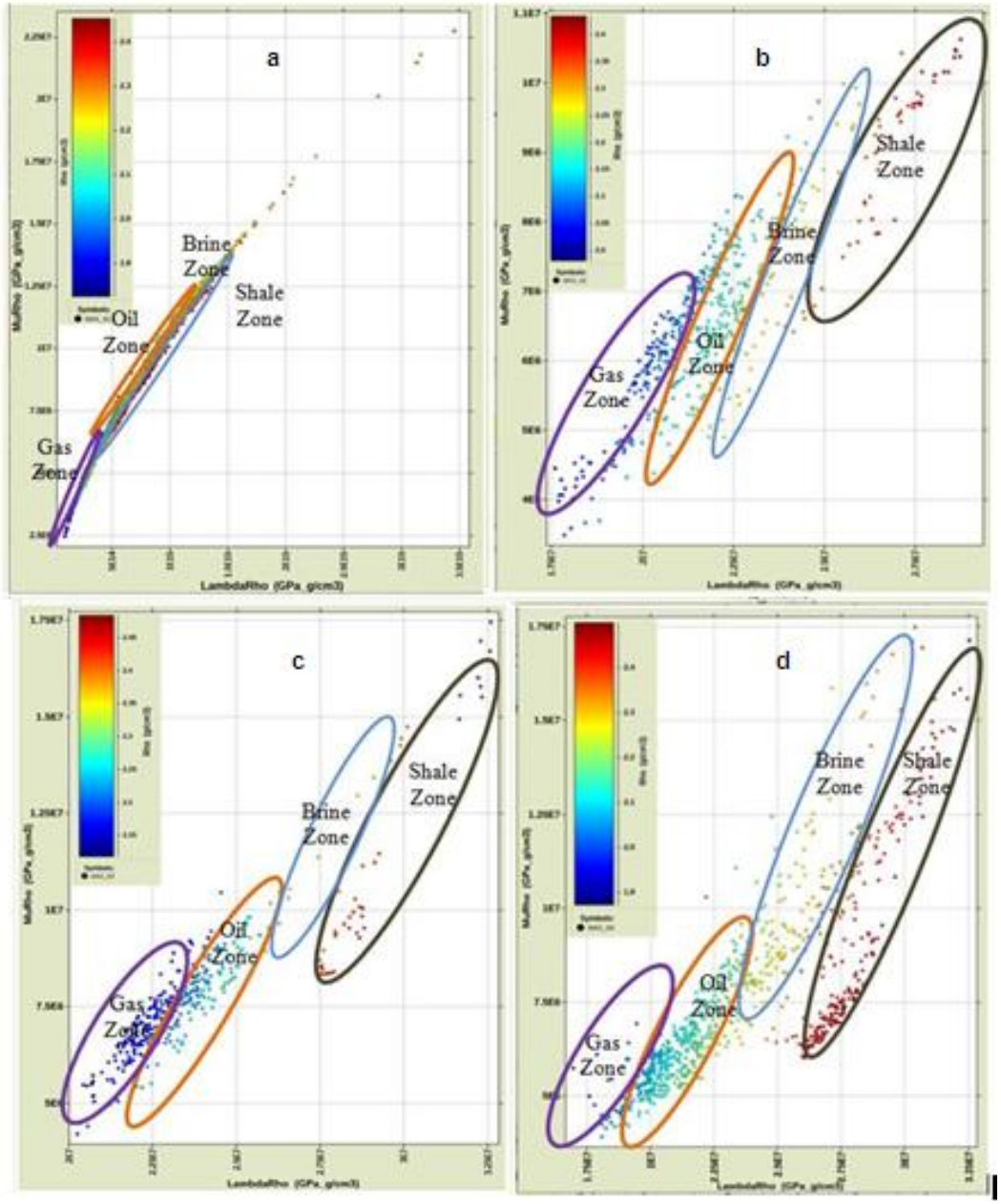

Fig. 20. Cross plot of Lambda-Rho (λρ) against Mu-Rho (μρ) color coded with Density for (a) HAX 01 (b) HAX 02 (c) HAX 03 (d) HAX 04

6. CONCLUSION

For this study, lithology delineation, well log correction, elastic properties estimation, and cross-plot analysis for fluid and lithology discrimination were all carried out. During well log correlation, three reservoir units were identified from lithology indicator logs like gamma ray, the presence of hydrocarbon was validated using high resistivity log signatures for reservoir zones while fluid discrimination to identify fluid type within the reservoir was done using the cross-plot of neutron against density. Fluid and lithology cross-plot analysis was also carried out with the reservoir of interest to discriminate fluid and lithology within that reservoir from the elastic rock properties estimated. These elastics rock properties include Lambda-Rho, Vp/Vs ratio, Acoustic Impedance, Mu-Rho, and Density. Hydrocarbon bearing reservoir zone was delineated and evaluated using cross-plot analysis, the reservoirs of interest R_5500, were

penetrated at depths 1935.22–2322.8m, 2177.54–2259.8m, 2229.51–2288.1m, 2136.76–2265.3m, and 2057.21–2663m across all wells respectively

For cross-plot analysis of some selected rock properties and attributes were carried out, Vp/Vs ratio against Acoustic Impedance, Lambda-Rho (λρ) against Vp/Vs, Mu-Rho against Density, and Lambda-Rho (λρ) against Mu-Rho (μρ) distinguished reservoir R_5500 into two zones namely sand zone and shale zone using the gamma ray has colour indictor for wells HAX 01, 02, 03, and 04 depicts that in the reservoirs the lithologies are majorly sands and shale predominantly found in Niger Delta. The cross-plot also showed the gamma ray colour-code affirming that the zone with the lowest values of Vp/Vs ratio, Lambda-Rho and P–Impedance with a little variation in Mu-Rho has the lowest gamma ray feedback, indicating that the zone is hydrocarbon bearing sand and the highest values of gamma ray concentrated indicates shale [3,41].

Conversely, the cross-plot of Vp/Vs ratio against Acoustic Impedance, Lambda-Rho (λρ) against Vp/Vs, Mu-Rho against Density and Lambda-Rho (λρ) against Mu-Rho (μρ) distinguished reservoir R_5500 into three zones namely hydrocarbon bearing zone, brine sand zone and shale zone using the water saturation has colour indicator for wells HAX 01, 02, 03, and 04 indicative of both lithology and fluid discrimination. From these cross-plots the clusters with the least water saturation correspond to highly charged hydrocarbon saturation sand while clusters with maximum water saturation correspond to non-hydrocarbon zone (brine sand and shale) [32,33].

And lastly, the cross-plot of Vp/Vs ratio against Acoustic Impedance, Lambda-Rho (λρ) against Vp/Vs, Mu-Rho against Density, and Lambda-Rho (λρ) against Mu-Rho (μρ) distinguished reservoir R_5500 into four zones namely gas sand zone and oil sand zone, brine sand zone, and shale zone using the density has colour indicator for wells HAX 01, 02, 03, and 04 depicts that in the reservoirs the fluid discriminates the shale (black ellipse), brine (blue ellipse), oil (orange ellipse) and gas (purple ellipse). In terms of fluid content, these attributes showed good discrimination since relatively lower Acoustic Impedance, Vp/Vs ratio, Lambda-Rho, Mu-Rho, and density (as the colour-code) values are indicative of hydrocarbon bearing sand while the relatively higher Acoustic Impedance, Vp/Vs ratio, Lambda-Rho, Mu-Rho, and density (as the colour-code) values are associated with non-hydrocarbon zone (shale and brine sand).

In conclusion, hydrocarbon-bearing sand (gas and oil) typically has low value readings from density, Acoustic Impedance, Lambda-Rho (λρ), Mu-Rho (μρ) (little variation), gamma ray and water saturation in Niger Delta than brine sand and shale. Therefore, brine sand and shale plots as medium to high property clusters in the cross plot space while hydrocarbon bearing sand (gas and oil) plots as low property clusters on Lambda-Rho (incompressibility) against Vp/Vs, Mu-Rho against Density and Lambda-Rho (λρ) against Mu-Rho (μρ) cross-plot space respectively.

This study has proven that the HAX field is viable in terms of hydrocarbon prospects within the reservoir of interest because the results of cross-plot analyses of elastic rock properties with reservoir properties were able to differentiate lithology and fluid within the reservoir of interest, therefore the field is said to be highly economical for production.

ACKNOWLEDGEMENTS

We are sincerely grateful to the DeGeoid Integrated Geoservices Limited their technical support

COMPETING INTERESTS

Authors have declared that no competing interests exist.

REFERENCES

1. Hami-Eddine K, Klein P, Loic R, Ribet B, Grout M. A new technique for lithology and fluid content prediction from prestack data: An application to carbonate reservoir. 2015;1.
2. Bello R, Igwenagu CL, Onifade YS. cross plotting of rock properties for fluid and lithology discrimination using well data in a Niger Delta oil field. J. Appl. Sci. Environ. Manage. 2015;19(3):538-546.
3. Udo KI, Akpabio IO, Umoren EB. Derived rock attributes analysis for enhanced reservoir fluid and lithology discrimination. IOSR Journal of Applied Geology and

Geophysics (IOSR-JAGG). 2017;5(2):95-105.

4. Akankpo AO, Umoren EB, Agbasi OE. Porosity estimation using wire-line log to depth in Niger Delta, Nigeria. Journal of Applied Geology and Geophysics. 2015; 3(4):31-38.
5. Brigaud F. Chapman FDS, Douaran SL. Estimating thermal conductivity in sedimentary basins using lithologic data and geophysical well logs. American Association of Petroleum Geologists Bulletin. 1990;74(9):1459–1477.
6. Inyang NJ, Okwueze EE, Agbasi OE. Detection of gas sands in the niger delta by estimation of poisson's dampening-factor (PDF) using wireline log data. Geosciences. 2015;5: 46-51.
DOI:10.5923/j.geo.20150501.06
7. Ellis DV. Singer JM. Well logging for earth scientists. Dordrecht, Netherlands, Springer, 692. 2008
8. Akpabio IO. Ojo OT. Characterization of hydrocarbon reservoir by pore fluid and lithology using elastic parameters in an X field, Niger Delta, Nigeria. International Journal of Advance Geosciences. 2018;6(2):173-177.
9. Ojo BT, Olowokere MT, Oladapo MI. Sensitivity analysis of changing reservoir saturation involving petrophysics and rock physics in 'Royal G' field, Niger Delta. Results in Geophysical Sciences; 2021. 100018.
10. Ojo BT, Olowokere MT, Oladapo MI. Quantitative modelling of the architecture and connectivity properties of reservoirs in 'Royal' Field, Niger-Delta. J. Appl. Geol. Geophys. 2018;6(2):01–10.
11. Bello R, Onifade YS. Discrimination of reservoir fluid contacts using compressional and shear wave velocity. Global Journal of Pure and Applied Sciences. 2016;22:177-190.
12. Okoli EA, Agbasi OE, Onyekuru S, Sunday EE. Cross plot analysis of rock properties from well log data for gas detection in Soku Field, coastal swamp depobelt, Niger Delta Basin. Journal of Geoscience, Engineering, Environment, and Technology. 2018;3(4).
13. Google Earth. Image Landsat/Copernicus; 2021.
14. Turtle MLW, Charpentier RR, Brownfield ME. The Niger Delta petroleum system: Niger Delta Province, Nigeria, Cameroun, and Equatorial Guinea, Africa. U.S.G.S. Open file Report. 1999;50 – 54.
15. Adeoti LA, Kolade A. Afinotan I. Fluid prediction using AVO analysis and forward modelling of deep reservoirs in Faith field, Niger Delta, Nigeria. Arabian Journal of Geosciences. 2014;8(6):4057–4074.
16. Doust H, Omatsola E. Niger Delta, in J.D. Edwards, and P.A. Santogrossi, Divergent/passive margin basins: American Association of Petroleum Geologists Memoir. 1990;48:201–238.
17. Ejedavwe J, Fatumbi A, Ladipo K, Stone K. Pan - Nigeria exploration well look - back (Post-Drill Well Analysis). Shell Petroleum Development Company of Nigeria Exploration Report; 2002.
18. Odunayo O, Okechukwu A, Inyang N, Sunday E, Ubong R. Prediction of pore fluid and lithology using incompressibility and rigidity, offshore Niger Delta, Nigeria. International Journal of Earth Sciences Knowledge and Applications. 2020;2(3):109-120.
19. Evamy BD, Haremboure J, Knaap P, Molloy FA, Rowlands PH. Hydrocarbon habitat of tertiary Niger Delta. American association of petroleum geologist. Bulletin. 1978;62:1–39.
20. Akpabio IO, Ibuot JC, Agbasi OE, Ojo OT. Petrophysical characterization of eight wells from wire-line logs, Niger Delta Nigeria. Asian Journal of Applied Science. 2014;2(2):105-109.
21. Ekweozor CM, Daukoru EM. Petroleum source bed evaluation of tertiary Niger Delta. American Association of Petroleum Geologists Bulletin. 1984;70:48-55,
22. Weber KJ, Daukoru EM. Petroleum geology of the Niger Delta. Ninth World Petroleum Congress. Tokyo. 1975;2:202–221,
23. Aigbadon GO, Babatunde GO, Aminu MB, Nanfa CA, Christopher SD. Depositional environments and reservoir evaluation of Otuma oil field, Niger - Delta basin, Nigeria. European Journal of Environment and Earth Sciences. 2021;2(6):53-57.
24. Adegoke OS, Oyebamiji AS, Edet JJ, Osterloff PL, Ulu OK. Cenozoic foraminifera and calcareous nannofossil biostratigraphy of the Niger Delta. Cathleen Sether, United States. 2017; 570.
25. Corredor F, Shaw JH, Bilotti F. Structural styles in the deep-water fold and thrust belts of the Niger Delta: American

Association of Petroleum Geologists Bulletin. 2005;89:753–780.
26. Lawrence SR, Munday S, Bray R. Regional geology and geophysics of the eastern Gulf of Guinea (Niger Delta to Rio Muni): The Leading Edge. 2002;21 (11):1112–1117.
27. Archie GE. The electrical resistivity log as an aid in determining some reservoir characteristics. Trans. 1942;54-62,
28. Castagna JP, Batzle ML, Eastwood RL. Relationships between compressional-wave and shear-wave velocities in clastic silicate rocks.Geophysics. 1985;50:571-581.
29. Omudu LM, Ebeniro JO, Osayande N, Adesanya S. Lithology and fluid discrimination from elastic rock properties cross plot: case study from Niger Delta. Proceeding, 24th Annual, International Conference and Exhibition of Petroleum Explorationist (NAPE) Abuja, Nigeria. 2006.
30. Goodway B, Chen T, Downton J. Improved AVO fluid detection and lithology discrimination using lame petrophysical parameters fluid stack from P and S – inversion. CSEG. 1997;148-151.
31. Alabi A, Enikanselu PA. Integrating seismic acoustic impedance inversion and attributes for reservoir analysis over 'DJ' Field, Niger Delta. J Petrol Explor Prod Technol. 2019;9(4):2487–2496.
32. Nssir NA, AL-Banna AS, Al-Sharaa GH. The using of Vp/Vs ratio and p-impedance for differentiate both fluid sand lithology depending on rock physics templates model of Mishrif and Nahr Umr formations in Kumait and Dujaila oil fields sothern Iraq. Bulletin of Pure and Applied Sciences, Geology (Geological Science). 2020;39F(2):285-300.
33. Abe SJ, Olowokere MT, Enikanselu PA. Development of model for predicting elastic parameters in 'bright' field, Niger Delta using rock physics analysis. NRIAG J. Astron. Geophys. 2018b;7(2):264–278.
34. Assefa S, McCan C, Sothcott J. Velocity of compressional and Shear waves in Limestone. Geophysical Prospecting. 2003;51(1):1-15.
35. Ebeniro JO, Dike RS, Udochu LO, Ezebilo, AA. Cross plotting and hydrocarbon indication in the Niger Delta. NAPE international conference and exhibitions, Abuja, Nigeria; 2003.
36. Oyetunji OO. Integrating rock physics and seismic inversion for reservoir characterization in the Gulf of Mexico. Masters Dissertation. University of Houston; 2013.
37. Abbey CP, Okpogo EU, Atueyi IO. Application of rock physics parameters for lithology and fluid prediction of 'TN' field of Niger Delta basin, Nigeria. Egyptian Journal of Petroleum. 2018;27:853–866.
38. Adeoti L, Allo OJ, Ayolabi EA, Akinmosin A, Oladele S, Oyeniran T, Ayuk MA. Reservoir fluid determination from angle stacked seismic volumes in 'Jay'field, Niger Delta, Nigeria. J Appl Sci Environ Manag. 2018;22(4):453–458.
39. Burianyk, M. Amplitude-versus-offset and seismic rock property analysis: A primer. CSEG Recorder. 2000;25(9):6–16.
40. Dewar J. Rock physics for the rest of us - an informal discussion. The Canadian Society of Exploration Geophysicist Recorder. 2001;5:43 – 4.
41. Dagogo T, Ehirim CN, Ebeniro JO. Enhanced prospect definition using well and 4D seismic data in a Niger Delta field. International Journal of Geosciences. 2016;7(8):977-990.

Peer-review history:
The peer review history for this paper can be accessed here:
https://www.sdiarticle5.com/review-history/98200